IEEE Access
Multidisciplinary | Rapid Review | Open Access Journal

Digital Object Identifier 10.1109/ACCESS.2021.DOI

LDPC Decoding with Low Complexity for OFDM Index Modulation

EUNCHUL YOON[1] (Senior Member, IEEE), SOONBUM KWON[1], UNIL YUN [2], and SUN-YONG KIM[1] (Senior Member, IEEE)

[1]Department of Electrical and Electronics Engineering at Konkuk University, Seoul, Korea (e-mail: ecyoon@konkuk.ac.kr; purusnorma@konkuk.ac.kr; kimsy@konkuk.ac.kr)
[2]Department of Computer Engineering at Sejong University, Seoul, Korea (e-mail: yunei@sejong.ac.kr)

Corresponding author: Sun-Yong Kim (e-mail: kimsy@konkuk.ac.kr).

This research was supported by Basic Science Research Program through the National Research Foundation of Korea (NRF) funded by the Ministry of Education (No.NRF-2018R1D1A1B07050232).

ABSTRACT In this paper, the posterior probabilities of the low-density parity check (LDPC) coded bits are derived for the orthogonal frequency division multiplexing index modulation (OFDM-IM) system to reduce the implementation complexity of LDPC decoding without performance loss. Specifically, the complexity of LDPC decoding is reduced by decomposing the posterior probability of the coded bit into multiple likelihood probabilities, each of which is obtained for each subcarrier of the corresponding OFDM-IM subblock. The results of the complexity analysis indicate that the proposed approach significantly reduces the implementation complexity of LDPC decoding for OFDM-IM compared to the conventional approach. Furthermore, the simulation results confirm that the proposed approach provides the same bit error rate performance as the conventional approach.

INDEX TERMS Communication system signaling, OFDM, decoding, index modulation, LDPC coding.

I. INTRODUCTION

INDEX modulation (IM) is a promising technology for 5G and beyond wireless networks to achieve additional data rates using indices of active resources, where resource can be any transmitting entities including transmit antennas, subcarriers, modulation types, precoders, time slots, and channel states [1]. A comprehensive overview of the existing IM framework and its principles are provided in [2]. The flexible use of existing IM techniques for 5G and beyond services was comprehensively examined in [3]. The concept of IM was merged with orthogonal frequency division multiplexing (OFDM) systems to design the subcarrier IM scheme (SIM) in [4] and it was called the OFDM-IM in [5]. The OFDM-IM conveys information bits through indices of active subcarriers in addition to those transmitted by data symbols, which helps achieve an increased spectral efficiency. Various OFDM-IM techniques have been proposed to further improve the spectral efficiency of OFDM-IM. In [6], OFDM-IM was applied independently to the in-phase/quadrature (IQ) components of each subcarrier, and was referred to as OFDM-IQ-IM in [7] and [8]. The dual mode OFDM-IM scheme (DM-OFDM-IM) was suggested in [9] and generalized to the generalized DM-OFDM-IM scheme in [10]. The multiple-mode OFDM-IM scheme (MM-OFDM-IM) and the multiple-mode OFDM-IQ-IM scheme (MM-OFDM-IQ-IM) were proposed in [11], wherein the full permutation of the symbol constellation modes was employed. Various OFDM-IM techniques have been developed to improve the bit error rate (BER) performance of OFDM-IM. In [12], subcarrier level interleaving was applied to OFDM-IM. In [13], the coordinate interleaved OFDM-IM (CI-OFDM-IM) was proposed, where interleaving was applied to the real and imaginary parts of every two complex symbols. In [7], the linear constellation precoding (LCP) technique was applied to OFDM-IQ-IM, and it was called LCP-OFDM-IQ-IM. In [8], the coordinate interleaving MM-OFDM-IM scheme and the LCP based MM-OFDM-IQ-IM scheme were proposed. Recently, OFDM-IM-based relay systems have gained considerable research attention. In [14], various frequency-domain IM schemes including OFDM-IM were introduced for cognitive radio (CR) networks and relay-aided networks. An OFDM-IM aided cooperative relay protocol for CR networks was studied in [15], where the secondary user transmitted its own data to the secondary receiver using indices of the active subcarriers of the primary user. The OFDM-IM-based CR scheme was investigated in [16] and [17]; in this scheme, the secondary user transmitted

its own data to the secondary receiver exploiting the inactive subcarriers of the primary user. A two-hop adaptive OFDM-IM relay protocol was proposed in [18], where the mapping between a bit stream and the indices of active subcarriers was selected adaptively based on the channel state information. A two-hop OFDM-IM relay protocol with multiple amplify-and-forward (AF) relays was studied in [20], and a multi-hop OFDM-IM relay protocol with multiple decode-and-forward relays was studied in [19]. In [21], a subcarrier/sub-channel mapping IM scheme was proposed for a dual-hop OFDM AF relay protocol, and it eliminated the overhead of transmitting SCM information.

To apply maximum likelihood (ML) detection for OFDM-IM, it is necessary to consider all possible subblock realizations, including all possible active subcarrier index combinations and symbol constellation points. Therefore, with a large subblock size and a high modulation order, ML detection becomes costly and infeasible for the practical implementation of the receiver. To reduce the complexity of ML detection for OFDM-IM, a reduced ML-detection was proposed in [5]. For the reduced ML detection, the indices of active subcarriers for each subblock were determined by searching for the maximum of the sum of the log likelihood ratios (LLRs). Then, the symbols transmitted over the active subcarriers were determined by applying ML detection. In [22], the use of reduced ML-detection was extended for the multiple-input multiple-output OFDM-IM scheme (MIMO-OFDM-IM) to develop minimum mean square error LLR (MMSE-LLR) detection. In [23], ordered successive interference cancellation based MMSE-LLR detection was proposed to further improve the error performance of MIMO-OFDM-IM. In [24], subblock-wise and subcarrier-wise detectors were proposed for MIMO-OFDM-IM, where the posterior probability of each subblock and each subcarrier were found iteratively based on the sequential Monte Carlo (SMC) theory. However, the subblock-wise detector had an exponentially increasing detection complexity with respect to the subblock size. The subcarrier-wise detector is preferred due to its low complexity, but its performance is inferior to that of the subblock-wise detector. Low-density parity check (LDPC) codes were applied for an OFDM-IM based in-vehicle power line communication system in [25] and for an MM-OFDM-IM system in [26]. Therein, the posterior probabilities of the index and data bits were provided and used as input for the LDPC decoder. While the formulas for calculating those posterior probabilities are applicable for any subblock size and modulation order, their practical application is limited to cases of a small subblock size and a low modulation order because of the computational complexity. Therefore, there is a need and a demand to develop a more efficient LDPC decoding approach for OFDM-IM with low computational complexity but no performance loss.

In this paper, the posterior probabilities of the LDPC-coded bits are derived for the OFDM-IM system to reduce the implementation complexity of LDPC decoding without performance loss. Since the LDPC-coded bits are delivered not only in the form of data symbols carried over the active subcarriers but also in the form of indices of the active subcarriers, the posterior probability of an index bit and that of a data bit are derived separately. The complexity of LDPC decoding is reduced by decomposing the posterior probability of the coded bit into multiple likelihood probabilities, each of which is obtained for each subcarrier of the corresponding OFDM-IM subblock. The results of the complexity analysis indicate that the proposed approach significantly reduces the implementation complexity of LDPC decoding for OFDM-IM compared to the conventional approach. Furthermore, the simulation results confirm that the proposed approach provides the same BER performance as the conventional approach.

The rest of this paper is organized as follows. Section II describes the system model of OFDM-IM. Section III derives the posterior probability of an index bit and that of a data bit separately. Section IV extends the proposed approach for higher-order modulation and analyzes the implementation complexity of the proposed and conventional approaches. Section V presents the simulation results and compares the BER performance of the proposed and conventional approaches. Finally, Section VI provides concluding remarks.

Notations: $(\cdot)^T$ and $(\cdot)^H$ stand for transpose and Hermitian transpose operations, respectively. $\lfloor x \rfloor$ denotes the greatest integer less than or equal to its argument. $|x|$ denotes the absolute value of a complex number x. $\mathrm{diag}(\mathbf{x})$ denotes a diagonal matrix with its diagonal components given by a vector $\mathbf{x}$. $\mathbf{x}(i)$ denotes the i-th component of a vector $\mathbf{x}$. $\mathcal{N}_x$ denotes a set given by $\{1, 2, \cdots, x\}$, where x is a natural number. $\mathrm{mod}(a, b)$ denotes the modulus function that returns the remainder when a is divided by b.

II. SYSTEM MODEL

Consider an LDPC-coded OFDM-IM system operating in a frequency-selective channel environment. The transmitter structure of the LDPC-coded OFDM-IM system is illustrated in Fig. 1. We assume that the OFDM block comprises N subcarriers and conveys N_I bits of information per OFDM block. In OFDM-IM, the OFDM block is divided into N_B subblocks. Each subblock has $n(= N/N_B)$ subcarriers, and transmits k M-ary QAM symbols over k active subcarriers. A message $\mathbf{m}$ consisting of N_I information bits is LDPC-coded to yield a codeword $\mathbf{c}'$ with N_C coded bits when the code rate is given by $R_C = N_I/N_C$. If $\mathbf{m}$ and $\mathbf{c}'$ are given in column vectors, $\mathbf{c}'$ can be written as

$$\mathbf{c}' = \mathbf{G}\mathbf{m}, \tag{1}$$

where $\mathbf{G}$ denotes an $N_C \times N_I$ dimensional systematic LDPC code generator matrix. If a sparse $(N_C - N_I) \times N_C$ dimensional parity check matrix $\mathbf{A}$ is ready, $\mathbf{G}$ can be computed as reported in [28, pp. 635]. The correctness of the estimated LDPC-coded bit vector $\hat{\mathbf{c}}'$ can be checked by the LDPC decoder based on $\mathbf{A}\hat{\mathbf{c}}' = 0$. The LDPC-coded bits of $\mathbf{c}'$ are

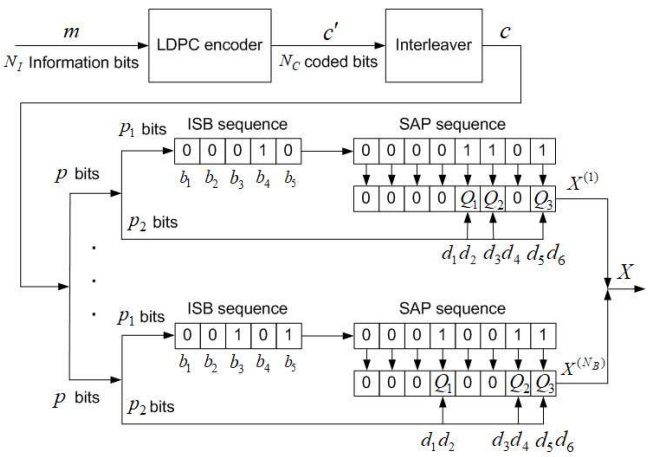

FIGURE 1. Transmitter structure of an LDPC-coded OFDM-IM system.

interleaved to yield $\mathbf{c}$. Then, $\mathbf{c}$ is divided into N_B sub-vectors as

$$\mathbf{c} = [\, \mathbf{c}_1^T \; \mathbf{c}_2^T \; \cdots \; \mathbf{c}_{N_B}^T \,]^T, \tag{2}$$

where each sub-vector of length $p = N_C/N_B$ is transmitted in a separate subblock. The first p_1 bits among the p bits are called the index selecting bits (ISBs) or index bits, and they are used to select the subcarrier activation pattern (SAP). The other $p_2(=p-p_1)$ bits among the p bits are called the symbol selecting bits or data bits, and they are used to choose k M-ary QAM symbols transmitted over k active subcarriers. An SAP can be written in a binary sequence comprising k 1's and $(n-k)$ 0's, which represent the active and inactive subcarriers, respectively. The total number of possible SAP candidate sequences is given by $N_{\text{SAP}} = {}_nC_k$, where ${}_nC_k$ denotes the number of the k combinations from a set of n components. Since each ISB sequence is associated with a separate SAP sequence, the value of p_1 can be selected as $p_1 = \lfloor \log_2(N_{\text{SAP}}) \rfloor$ for maximal spectral efficiency. In the case that $N_{\text{SAP}} > 2^{p_1}$, 2^{p_1} SAP sequences need to be selected from N_{SAP} SAP candidate sequences for a one-to-one mapping between the ISB and SAP sequences. We assume that the mapping between the ISB and SAP sequences is based on combinational mapping [5]. For $i = 1, 2, \cdots, 2^{p_1}$, we define the i-th binary sequence of length p_1 corresponding to a decimal number $i-1$ as

$$\mathbf{V}_i = [\, v_{i,1} \; v_{i,2} \; \cdots \; v_{i,p_1} \,], \tag{3}$$

where $v_{i,1}$ and v_{i,p_1} denote the most significant bit (MSB) and least significant bit (LSB), respectively, while $v_{i,l} \in \{0,1\}$ for $l = 1, 2, \cdots, p_1$. The ISB sequences $\{\mathbf{ISB}_\eta\}_{\eta=1}^{2^{p_1}}$ are defined as $\mathbf{ISB}_i = \mathbf{V}_i$ for $i = 1, 2, \cdots, 2^{p_1}$. For $i = 1, 2, \cdots, 2^n$, we define the i-th binary sequence of length n corresponding to a decimal number $i-1$ as

$$\mathbf{Z}_i = [\, z_{i,1} \; z_{i,2} \; \cdots \; z_{i,n} \,], \tag{4}$$

where $z_{i,1}$ and $z_{i,n}$ denote the MSB and LSB, respectively, while $z_{i,l} \in \{0,1\}$ for $l = 1, 2, \cdots, n$. The SAP sequences $\{\mathbf{a}_\eta\}_{\eta=1}^{2^{p_1}}$ are generated by selecting the first 2^{p_1} sequences that have k 1's and $(n-k)$ 0's from $\{\mathbf{Z}_\eta\}_{\eta=1}^{2^n}$. The η-th SAP sequence is written as

$$\mathbf{a}_\eta = [\, a_{\eta,1}, a_{\eta,2}, \cdots, a_{\eta,n} \,], \tag{5}$$

where $a_{\eta,m} \in \{0,1\}$ for $m = 1, 2, \cdots, n$. We define a set of k active subcarrier indices in the η-th SAP sequence as

$$\mathcal{I}^{(\eta)} = \{ I_1^{(\eta)}, I_2^{(\eta)}, \cdots, I_k^{(\eta)} \} \tag{6}$$

for $\eta = 1, 2, \cdots, 2^{p_1}$, where $I_1^{(\eta)}, I_2^{(\eta)}, \cdots, I_k^{(\eta)} \in \mathcal{N}_n$. According to combinational mapping [5], the i-th ISB sequence is mapped to the i-th SAP sequence for $i = 1, 2, \cdots, 2^{p_1}$, i.e., $\{\mathbf{ISB}_\eta\}_{\eta=1}^{2^{p_1}}$ are associated with $\{\mathbf{a}_\eta\}_{\eta=1}^{2^{p_1}}$ in consecutive order. The OFDM block is written as

$$\mathbf{X} = [\, \mathbf{X}^{(1)^T} \; \mathbf{X}^{(2)^T} \; \cdots \; \mathbf{X}^{(N_B)^T} \,]^T, \tag{7}$$

where $\mathbf{X}^{(\beta)}$ denotes the β-th subblock,

$$\mathbf{X}^{(\beta)} = [\, X_1^{(\beta)} \; X_2^{(\beta)} \; \cdots \; X_n^{(\beta)} \,]^T, \tag{8}$$

while $X_v^{(\beta)}$ denotes the v-th symbol of the β-th subblock. Since a subcarrier-level interleaver improves error performance by transforming a frequency domain channel into an uncorrelated one [12], we assume that $\mathbf{X}$ passes through a symbol-level interleaver to yield

$$\tilde{\mathbf{X}} = [\, X_1^{(1)} \cdots X_1^{(N_B)} \; X_2^{(1)} \cdots X_2^{(N_B)} \; \cdots X_n^{(1)} \cdots X_n^{(N_B)} \,]^T. \tag{9}$$

The interleaved OFDM block $\tilde{\mathbf{X}}$ undergoes inverse fast Fourier transform and cyclic prefix addition before transmission. The frequency-selective channel is modeled as a tapped delay-line of length L as

$$\mathbf{h} = [\, h_1 \; h_2 \; \cdots \; h_L \,]^T. \tag{10}$$

Channel coefficients $\{h_l\}_{l=1}^{L}$ are assumed to be uncorrelated with each other and have a zero-mean circularly symmetric complex Gaussian distribution. The average power of h_l is given by

$$E\{|h_l|^2\} = \frac{\gamma^{l-1}}{\sum_{l'=1}^{L} \gamma^{l'-1}}, \tag{11}$$

where γ denotes a power delay profile factor in the range of $0 < \gamma \leq 1$. In simulation, γ is set to 0.9. At the receiver, a series of processes including cyclic prefix elimination, fast Fourier transform, and subcarrier-level de-interleaving are applied to the received signal. Then, the received signal for the β-th subblock can be written as

$$\mathbf{Y}^{(\beta)} = \text{diag}\big(\mathbf{H}^{(\beta)}\big)\mathbf{X}^{(\beta)} + \mathbf{W}^{(\beta)}, \tag{12}$$

where $\mathbf{H}^{(\beta)}$ denotes the frequency domain channel vector

$$\mathbf{H}^{(\beta)} = [\, H_1^{(\beta)} \; H_2^{(\beta)} \; \cdots \; H_n^{(\beta)} \,]^T, \tag{13}$$

with its component given by

$$H_m^{(\beta)} = \sum_{l=1}^{L} h_l e^{-j\frac{2\pi}{N} \times (l-1) \times ((\beta-1)n+m-1))}. \tag{14}$$

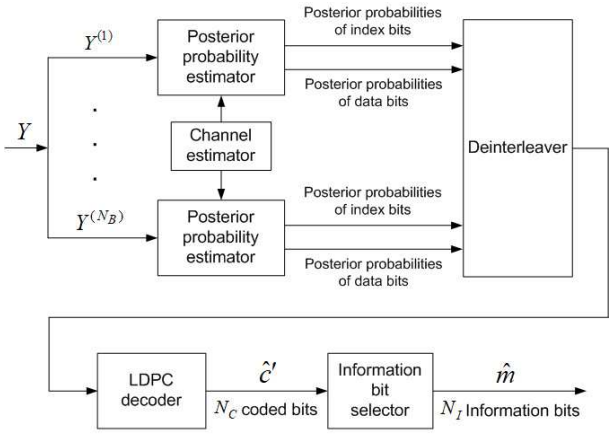

FIGURE 2. Receiver structure of an LDPC-coded OFDM-IM system.

$\mathbf{W}^{(\beta)}$ denotes an additive noise vector

$$\mathbf{W}^{(\beta)} = \left[W_1^{(\beta)} \; W_2^{(\beta)} \; \cdots \; W_n^{(\beta)} \right]^T, \tag{15}$$

with $W_m^{(\beta)}$ indicating a zero-mean circularly symmetric complex Gaussian random variable with variance N_0. The signal-to-noise ratio (SNR) is defined as $\rho = E_b/N_0$, where E_b denotes the average energy per bit. We define $\mathcal{S}$ as the set that contains all symbols of an M-ary QAM constellation. If $\mathbf{X}^{(\beta)}$ is subjected to the η-th SAP sequence, $X_v^{(\beta)}$ corresponds to a symbol belonging to $\mathcal{S}$ when $v \in \mathcal{I}^{(\eta)}$ and 0 when $v \notin \mathcal{I}^{(\eta)}$. $\mathbf{Y}^{(\beta)}$ in (12) can be rewritten as

$$\mathbf{Y}^{(\beta)} = [\, Y_1^{(\beta)} \; Y_2^{(\beta)} \cdots \; Y_n^{(\beta)} \,]^T, \tag{16}$$

where $Y_v^{(\beta)}$ is given by

$$Y_v^{(\beta)} = H_v^{(\beta)} X_v^{(\beta)} + W_v^{(\beta)}. \tag{17}$$

The receiver structure of the LDPC-coded OFDM-IM system is illustrated in Fig. 2. We separate the posterior probability estimator block from the LDPC decoder block to modularize the entire LDPC decoding process. Due to modularity, the LDPC decoder block in Fig. 2 can be replaced with other decoder blocks to apply different codes in the condition that the decoder takes posterior probabilities as input. When it comes to Turbo decoding, the BCJR decoding algorithm [27] is commonly used. Since the BCJR decoding algorithm requires likelihood probabilities as input instead of posterior probabilities, the LDPC decoder block in Fig. 2 cannot be replaced by the conventional turbo decoder block for turbo code application. With OFDM-IM, symbols carried over different subcarriers within each subblock are bound together because of IM. Considering this boundness effect, in the next section, we derive the posterior probabilities of the LDPC-coded bits as simple as possible to reduce the implementation complexity of the entire LDPC decoding process. The channel frequency response (CFR) coefficient over the subcarrier of the p-th pilot symbol for $p = 0, 1, \cdots, N_P - 1$ is estimated by the least square detection method [29], where N_P denotes the number of pilot symbols in an OFDM block. The CFR coefficients over non-pilot subcarriers are estimated by applying the MMSE-based channel interpolation method [30]. For LDPC decoding, the posterior probability estimator computes the posterior probabilities of the LDPC-coded bits in the β-th subblock using the information of $\{Y_v^{(\beta)}\}_{v=1}^n$ and $\{\hat{H}_v^{(\beta)}\}_{v=1}^n$, where $\hat{H}_v^{(\beta)}$ denotes the CFR coefficient estimated at the receiver. The posterior probabilities from all subblocks are gathered and deinterleaved. Using the deinterleaved posterior probabilities as input, the LDPC decoder yields the estimated LDPC-coded bit vector $\hat{\mathbf{c}}'$ based on the sum-product decoding algorithm (SPA) [28, p. 648]. The SPA runs a decoding loop where a temporary $\hat{\mathbf{c}}'$ vector is updated iteratively. The correctness of the temporary $\hat{\mathbf{c}}'$ in the decoding loop is confirmed by the parity check condition $\mathbf{A}\hat{\mathbf{c}}' = 0$. If $\mathbf{A}\hat{\mathbf{c}}' \neq 0$, the decoding loop continues. If the maximum number of iterations is reached, a decoding failure is declared and the iteration process is stopped. If $\mathbf{A}\hat{\mathbf{c}}' = 0$, the decoding loop is stopped and the estimated message $\hat{\mathbf{m}}$ is given by

$$\hat{\mathbf{m}} = [\, \hat{\mathbf{c}}'(N_C - N_I + 1) \; \hat{\mathbf{c}}'(N_C - N_I + 2) \; \cdots \; \hat{\mathbf{c}}'(N_C) \,]^T \tag{18}$$

because of systematic structure of the generator matrix $\mathbf{G}$.

III. PROPOSED APPROACH

We focus on the β-th subblock to derive the posterior probabilities of the LDPC-coded bits because each subblock is subject to the same OFDM-IM procedure. We define $Q_1, Q_2, \cdots, Q_k$ as the k M-ary QAM symbols carried over the k active subcarriers of the β-th subblock. We define a number $D = \log_2(M)$ to denote the number of data bits delivered in a single M-ary QAM symbol. Then, the number of data bits delivered in the β-th subblock is given by $p_2 = k \times D$. We define $b_1, \; b_2, \; \cdots, \; b_{p_1}$ in consecutive order as the p_1 index bits used for selecting an ISB sequence. Furthermore, we define $d_1, \; d_2, \; \cdots, \; d_{p_2}$ in consecutive order as the p_2 data bits used for selecting $Q_1, \; Q_2, \cdots, Q_k$. For the convenience of illustration, we focus on a specific OFDM-IM system with $n = 8$, $k = 3$, $D = 2$, $p_1 = 5$, $p_2 = 6$, and $N_{\text{SAP}} = 56$, when 4QAM symbols are used as the transmitted symbols. The proposed approach, in which the posterior probabilities of the index and data bits are formulated as simple as possible, can also be applied to other OFDM-IM systems with other parameters, such as a larger subblock size and a higher modulation order. We define a set of 4QAM symbols as

$$\mathcal{S} = \{s_{0,0}, \; s_{0,1}, \; s_{1,0}, \; s_{1,1}\}, \tag{19}$$

where the values of the four components in $\mathcal{S}$ are determined by Gray mapping [31]. An example of Gray mapping is given by $s_{0,0} = (1 + j)/\sqrt{2}, s_{0,1} = (-1 + j)/\sqrt{2}, s_{1,0} = (1 - j)/\sqrt{2}$, and $s_{1,1} = (-1 - j)/\sqrt{2}$. We define $2p_2$ subsets of $\mathcal{S}$ as

$$\mathcal{S}_{i,x} = \begin{cases} \Phi_{1,x} & \text{if } \text{mod}(i, D) = 1 \\ \Phi_{2,x} & \text{if } \text{mod}(i, D) = 0 \end{cases} \tag{20}$$

for $i = 1, 2, \cdots, p_2$, and $x \in \{0, 1\}$, where

$$\Phi_{1,x} = \{s_{x,0}, s_{x,1}\}, \tag{21}$$

$$\Phi_{2,x} = \{s_{0,x}, s_{1,x}\}. \tag{22}$$

In addition, we set the values of $Q_1, Q_2, \cdots, Q_k$ as

$$Q_{\lfloor (i+D-1)/D \rfloor} = \begin{cases} s_{d_i, d_{i+1}} & \text{if mod}(i, D) = 1 \\ s_{d_{i-1}, d_i} & \text{if mod}(i, D) = 0 \end{cases} \tag{23}$$

for $i = 1, 2, \cdots, p_2$. Given $d_i = x$, $\mathcal{S}_{i,x}$ corresponds to the set of all symbols suitable for $Q_{\lfloor (i+D-1)/D \rfloor}$.

A. DERIVATION OF THE POSTERIOR PROBABILITY OF AN INDEX BIT

We define $\mathcal{A}$ as the set of all SAP sequences $\{\mathbf{a}_\eta\}_{\eta=1}^{2^{p_1}}$. In addition, we define $\mathcal{A}_{b_i=x}$ as the set of all SAP sequences that satisfy the condition $b_i = x$ for $i = 1, 2, \cdots, p_1$ and $x \in \{0, 1\}$. Applying the total probability rule, we write the posterior probability of $b_i = x$ given $\mathbf{Y}^{(\beta)}$ as

$$p(b_i = x|\mathbf{Y}^{(\beta)}) = \sum_{\mathbf{a}_\eta \in \mathcal{A}_{b_i=x}} p(b_i = x, \mathbf{a}_\eta|\mathbf{Y}^{(\beta)}) \tag{24}$$

for $i = 1, 2, \cdots, p_1$ and $x \in \{0, 1\}$. Using Bayes' rule, we derive the posterior probability of $p(b_i = x, \mathbf{a}_\eta|\mathbf{Y}^{(\beta)})$ in terms of the likelihood probability of $p(\mathbf{Y}^{(\beta)}|\mathbf{a}_\eta, b_i = x)$ as

$$p(b_i = x, \mathbf{a}_\eta|\mathbf{Y}^{(\beta)}) = \frac{p(\mathbf{a}_\eta)p(b_i = x|\mathbf{a}_\eta)p(\mathbf{Y}^{(\beta)}|\mathbf{a}_\eta, b_i = x)}{p(\mathbf{Y}^{(\beta)})}. \tag{25}$$

Since $\mathbf{a}_\eta \in \mathcal{A}_{b_i=x}$, it follows that $p(\mathbf{a}_\eta) = 1/2^{p_1-1}$, $p(b_i = x|\mathbf{a}_\eta) = 1$, and $p(\mathbf{Y}^{(\beta)}|\mathbf{a}_\eta, b_i = x) = p(\mathbf{Y}^{(\beta)}|\mathbf{a}_\eta)$. Therefore, we can write (24) as

$$p(b_i = x|\mathbf{Y}^{(\beta)}) = \frac{1}{2^{p_1-1}p(\mathbf{Y}^{(\beta)})} \sum_{\mathbf{a}_\eta \in \mathcal{A}_{b_i=x}} p(\mathbf{Y}^{(\beta)}|\mathbf{a}_\eta). \tag{26}$$

Since the components of $\mathbf{Y}^{(\beta)}$ given $\mathbf{a}_\eta$ are independent of each other in the case of $\mathbf{a}_\eta \in \mathcal{A}_{b_i=x}$, we obtain

$$p(b_i = x|\mathbf{Y}^{(\beta)}) = \frac{1}{2^{p_1-1}p(\mathbf{Y}^{(\beta)})} \sum_{\mathbf{a}_\eta \in \mathcal{A}_{b_i=x}} \prod_{m \in \mathcal{N}_n} p(Y_m^{(\beta)}|\mathbf{a}_\eta). \tag{27}$$

Considering the condition $\mathbf{a}_\eta \in \mathcal{A}_{b_i=x}$, we divide the probabilities $\{p(Y_m^{(\beta)}|\mathbf{a}_\eta)\}_{m \in \mathcal{N}_n}$ into two groups; the first group comprises the probabilities of $Y_m^{(\beta)}$ given $\mathbf{a}_\eta$ for $b_i = x$ and $m \in \mathcal{I}^{(\eta)}$, and the second group comprises the probabilities of $Y_m^{(\beta)}$ given $\mathbf{a}_\eta$ for $b_i = x$ and $m \notin \mathcal{I}^{(\eta)}$. Using this grouping, we obtain

$$\prod_{m \in \mathcal{N}_n} p(Y_m^{(\beta)}|\mathbf{a}_\eta) = \prod_{m \in \mathcal{I}^{(\eta)}} p(Y_m^{(\beta)}|\mathbf{a}_\eta) \prod_{m \in \mathcal{N}_n,\, m \notin \mathcal{I}^{(\eta)}} p(Y_m^{(\beta)}|\mathbf{a}_\eta). \tag{28}$$

Applying the total probability and Bayes' rules to the term $\prod_{m \in \mathcal{I}^{(\eta)}} p(Y_m^{(\beta)}|\mathbf{a}_\eta)$ in (28), we write

$$\prod_{m \in \mathcal{I}^{(\eta)}} p(Y_m^{(\beta)}|\mathbf{a}_\eta) = \prod_{m \in \mathcal{I}^{(\eta)}} \frac{1}{M} \sum_{s \in \mathcal{S}} p(Y_m^{(\beta)}|X_m^{(\beta)} = s, \mathbf{a}_\eta), \tag{29}$$

where the assumption of $p(X_m^{(\beta)} = s|\mathbf{a}_\eta) = 1/M$ for $m \in \mathcal{I}^{(\eta)}$ and $s \in \mathcal{S}$ is used. The event of $Y_m^{(\beta)}$ given $X_m^{(\beta)} = s$ and $\mathbf{a}_\eta$ for $m \in \mathcal{I}^{(\eta)}$ and $s \in \mathcal{S}$ follows a Gaussian distribution

$$p(Y_m^{(\beta)}|X_m^{(\beta)} = s, \mathbf{a}_\eta) = \frac{1}{\pi N_0} e^{-\frac{\left|Y_m^{(\beta)} - H_m^{(\beta)} s a_{\eta,m}\right|^2}{N_0}}. \tag{30}$$

Therefore, we derive

$$\prod_{m \in \mathcal{I}^{(\eta)}} p(Y_m^{(\beta)}|\mathbf{a}_\eta) = \prod_{m \in \mathcal{I}^{(\eta)}} \frac{1}{\pi N_0 M} \sum_{s \in \mathcal{S}} e^{-\frac{\left|Y_m^{(\beta)} - H_m^{(\beta)} s a_{\eta,m}\right|^2}{N_0}}. \tag{31}$$

Since $p(Y_m^{(\beta)}|\mathbf{a}_\eta) = p(Y_m^{(\beta)}, X_m^{(\beta)} = 0|\mathbf{a}_\eta)$ for $m \notin \mathcal{I}^{(\eta)}$, we can write the term $\prod_{m \in \mathcal{N}_n, m \notin \mathcal{I}^{(\eta)}} p(Y_m^{(\beta)}|\mathbf{a}_\eta)$ in (28) as

$$\prod_{m \in \mathcal{N}_n, m \notin \mathcal{I}^{(\eta)}} p(Y_m^{(\beta)}|\mathbf{a}_\eta) = \prod_{m \in \mathcal{N}_n, m \notin \mathcal{I}^{(\eta)}} p(Y_m^{(\beta)}, X_m^{(\beta)} = 0|\mathbf{a}_\eta). \tag{32}$$

Applying Bayes' rule to (32), we obtain

$$\prod_{m \in \mathcal{N}_n,\, m \notin \mathcal{I}^{(\eta)}} p(Y_m^{(\beta)}|\mathbf{a}_\eta) = \prod_{m \in \mathcal{N}_n,\, m \notin \mathcal{I}^{(\eta)}} p(Y_m^{(\beta)}|X_m^{(\beta)} = 0, \mathbf{a}_\eta), \tag{33}$$

where the assumption of $p(X_m^{(\beta)} = 0|\mathbf{a}_\eta) = 1$ for $m \notin \mathcal{I}^{(\eta)}$ is used. The event of $Y_m^{(\beta)}$ given $X_m^{(\beta)} = 0$ and $\mathbf{a}_\eta$ for $m \notin \mathcal{I}^{(\eta)}$ follows a Gaussian distribution

$$p(Y_m^{(\beta)}|X_m^{(\beta)} = 0, \mathbf{a}_\eta) = \frac{1}{\pi N_0} e^{-\frac{\left|Y_m^{(\beta)}\right|^2}{N_0}}. \tag{34}$$

Since $a_{\eta,m} = 0$ for $m \notin \mathcal{I}^{(\eta)}$, we can write (34) as

$$p(Y_m^{(\beta)}|X_m^{(\beta)} = 0, \mathbf{a}_\eta) = \frac{1}{\pi N_0 M} \sum_{s \in \mathcal{S}} e^{-\frac{\left|Y_m^{(\beta)} - H_m^{(\beta)} s a_{\eta,m}\right|^2}{N_0}}. \tag{35}$$

Substituting the result of (35) into (33), we derive

$$\prod_{m \in \mathcal{N}_n,\, m \notin \mathcal{I}^{(\eta)}} p(Y_m^{(\beta)}|\mathbf{a}_\eta) = \prod_{m \in \mathcal{N}_n,\, m \notin \mathcal{I}^{(\eta)}} \frac{1}{\pi N_0 M} \sum_{s \in \mathcal{S}} e^{-\frac{\left|Y_m^{(\beta)} - H_m^{(\beta)} s a_{\eta,m}\right|^2}{N_0}}. \tag{36}$$

Substituting the result of (31) and (36) into (28) and then substituting the result of (28) into (27), we obtain

$$p(b_i = x|\mathbf{Y}^{(\beta)}) = C_1 \sum_{\mathbf{a}_\eta \in \mathcal{A}_{b_i=x}} \prod_{m \in \mathcal{N}_n} \sum_{s \in \mathcal{S}} e^{-\frac{\left|Y_m^{(\beta)} - H_m^{(\beta)} s\, a_{\eta,m}\right|^2}{N_0}}, \tag{37}$$

where C_1 denotes a normalization constant that satisfies

$$p(b_i = 1|\mathbf{Y}^{(\beta)}) + p(b_i = 0|\mathbf{Y}^{(\beta)}) = 1. \tag{38}$$

Taking the $\ln(\cdot)$ function on both sides of (37) and then applying the approximation property [32]

$$\ln\left\{\sum_z e^{-f(z)}\right\} \approx -\min_z f(z), \tag{39}$$

This article has been accepted for publication in a future issue of this journal, but has not been fully edited. Content may change prior to final publication. Citation information: DOI 10.1109/ACCESS.2021.3077256, IEEE Access

we obtain

$$\ln\{p(b_i = x|\mathbf{Y}^{(\beta)})\} \approx \ln(C_1) - \min_{\mathbf{a}_\eta \in \mathcal{A}_{b_i=x}} \sum_{m\in\mathcal{N}_n} \min_{s\in\mathcal{S}} \frac{|Y_m^{(\beta)} - H_m^{(\beta)} s\, a_{\eta,m}|^2}{N_0}. \quad (40)$$

The LLR of the index bit b_i for $i = 1, 2, \cdots, p_1$ is

$$\lambda_i = \ln\{p(b_i = 1|\mathbf{Y}^{(\beta)})\} - \ln\{p(b_i = 0|\mathbf{Y}^{(\beta)})\}. \quad (41)$$

The term $\ln(C_1)$ in (40) does not have to be considered for the computation of λ_i in (41). Based on (40) and (41), we derive the LLR of the index bit b_i for $i = 1, 2, \cdots, p_1$ as

$$\lambda_i = \min_{\mathbf{a}_\eta \in \mathcal{A}_{b_i=0}} \sum_{m\in\mathcal{N}_n} \min_{s\in\mathcal{S}} \frac{|Y_m^{(\beta)} - H_m^{(\beta)} s\, a_{\eta,m}|^2}{N_0} - \min_{\mathbf{a}_\eta \in \mathcal{A}_{b_i=1}} \sum_{m\in\mathcal{N}_n} \min_{s\in\mathcal{S}} \frac{|Y_m^{(\beta)} - H_m^{(\beta)} s\, a_{\eta,m}|^2}{N_0}. \quad (42)$$

Given λ_i, the posterior probabilities of $p(b_i = 1|\mathbf{Y}^{(\beta)})$ and $p(b_i = 0|\mathbf{Y}^{(\beta)})$ can be computed by

$$p(b_i = 1|\mathbf{Y}^{(\beta)}) = \frac{1}{e^{-\lambda_i} + 1} \quad (43)$$

and

$$p(b_i = 0|\mathbf{Y}^{(\beta)}) = 1 - p(b_i = 1|\mathbf{Y}^{(\beta)}). \quad (44)$$

B. DERIVATION OF THE POSTERIOR PROBABILITY OF A DATA BIT

Applying the total probability rule, we write the posterior probability of $d_i = x$ given $\mathbf{Y}^{(\beta)}$ as

$$p(d_i = x|\mathbf{Y}^{(\beta)}) = \sum_{\eta=1}^{2^{p_1}} p(d_i = x, \mathbf{a}_\eta|\mathbf{Y}^{(\beta)}) \quad (45)$$

for $i = 1, 2, \cdots, p_2$ and $x \in \{0, 1\}$. Using Bayes' rule, we derive the posterior probability of $p(d_i = x, \mathbf{a}_\eta|\mathbf{Y}^{(\beta)})$ in terms of the likelihood probability of $p(\mathbf{Y}^{(\beta)}|\mathbf{a}_\eta, d_i = x)$ as

$$p(d_i = x, \mathbf{a}_\eta|\mathbf{Y}^{(\beta)}) = \frac{p(\mathbf{a}_\eta)p(d_i = x|\mathbf{a}_\eta)p(\mathbf{Y}^{(\beta)}|\mathbf{a}_\eta, d_i = x)}{p(\mathbf{Y}^{(\beta)})}. \quad (46)$$

Since $p(\mathbf{a}_\eta) = 1/2^{p_1}$ and $p(d_i = x|\mathbf{a}_\eta) = p(d_i = x) = 1/2$, we can write (45) as

$$p(d_i = x|\mathbf{Y}^{(\beta)}) = \frac{1}{2^{p_1+1}p(\mathbf{Y}^{(\beta)})} \sum_{\eta=1}^{2^{p_1}} p(\mathbf{Y}^{(\beta)}|\mathbf{a}_\eta, d_i = x). \quad (47)$$

Since the components of $\mathbf{Y}^{(\beta)}$ given $\mathbf{a}_\eta$ and $d_i = x$ are independent of each other, we obtain

$$p(\mathbf{Y}^{(\beta)}|\mathbf{a}_\eta, d_i = x) = \prod_{m\in\mathcal{N}_n} p(Y_m^{(\beta)}|\mathbf{a}_\eta, d_i = x). \quad (48)$$

The event of $Y_m^{(\beta)}$ given $\mathbf{a}_\eta$ and $d_i = x$ follows a Gaussian distribution

$$p(Y_m^{(\beta)}|\mathbf{a}_\eta, d_i = x) = \sum_{s\in\Psi_{m,i,x}} \frac{1}{\pi N_0} e^{-\frac{\left|Y_m^{(\beta)} - H_m^{(\beta)} s a_{\eta,m}\right|^2}{N_0}}, \quad (49)$$

where

$$\Psi_{m,i,x} = \begin{cases} S_{i,x} & \text{if } m = I^{(\eta)}_{\lfloor (i+D-1)/D \rfloor} \\ \mathcal{S} & \text{if } m \in \mathcal{I}^{(\eta)},\ m \neq I^{(\eta)}_{\lfloor (i+D-1)/D \rfloor} \\ \{0\} & \text{if } m \in \mathcal{N}_n,\ m \notin \mathcal{I}^{(\eta)} \end{cases}. \quad (50)$$

Substituting the result of (49) into (48) and then substituting the result of (48) into (47), we obtain

$$p(d_i = x|\mathbf{Y}^{(\beta)}) = C_2 \sum_{\eta=1}^{2^{p_1}} \left\{ \left(\sum_{s\in\mathcal{S}_{i,x}} e^{-\frac{\left|Y^{(\beta)}_{I^{(\eta)}_{\lfloor (i+D-1)/D \rfloor}} - H^{(\beta)}_{I^{(\eta)}_{\lfloor (i+D-1)/D \rfloor}} s\right|^2}{N_0}} \right) \times \prod_{m\in\mathcal{N}_n, m\neq I^{(\eta)}_{\lfloor (i+D-1)/D \rfloor}} \sum_{s\in\mathcal{S}} e^{-\frac{\left|Y_m^{(\beta)} - H_m^{(\beta)} s a_{\eta,m}\right|^2}{N_0}} \right\}, \quad (51)$$

where C_2 denotes a normalization constant that satisfies

$$p(d_i = 1|\mathbf{Y}^{(\beta)}) + p(d_i = 0|\mathbf{Y}^{(\beta)}) = 1. \quad (52)$$

The LLR of the data bit d_i for $i = 1, 2, \cdots, p_2$ is

$$\bar{\lambda}_i = \ln\{p(d_i = 1|\mathbf{Y}^{(\beta)})\} - \ln\{p(d_i = 0|\mathbf{Y}^{(\beta)})\}. \quad (53)$$

Taking the $\ln(\cdot)$ function on both sides of (51) and then applying the approximation property of (39), we derive the LLR of the data bit d_i for $i = 1, 2, \cdots, p_2$ as

$$\bar{\lambda}_i = \min_{\eta\in\mathcal{N}_{2^{p_1}}} \left\{ \min_{s\in\mathcal{S}_{i,0}} \frac{\left|Y^{(\beta)}_{I^{(\eta)}_{\lfloor (i+D-1)/D \rfloor}} - H^{(\beta)}_{I^{(\eta)}_{\lfloor (i+D-1)/D \rfloor}} s\right|^2}{N_0} + \sum_{m\in\mathcal{N}_n, m\neq I^{(\eta)}_{\lfloor (i+D-1)/D \rfloor}} \min_{s\in\mathcal{S}} \frac{\left|Y_m^{(\beta)} - H_m^{(\beta)} s\, a_{\eta,m}\right|^2}{N_0} \right\} - \min_{\eta\in\mathcal{N}_{2^{p_1}}} \left\{ \min_{s\in\mathcal{S}_{i,1}} \frac{\left|Y^{(\beta)}_{I^{(\eta)}_{\lfloor (i+D-1)/D \rfloor}} - H^{(\beta)}_{I^{(\eta)}_{\lfloor (i+D-1)/D \rfloor}} s\right|^2}{N_0} + \sum_{m\in\mathcal{N}_n, m\neq I^{(\eta)}_{\lfloor (i+D-1)/D \rfloor}} \min_{s\in\mathcal{S}} \frac{\left|Y_m^{(\beta)} - H_m^{(\beta)} s\, a_{\eta,m}\right|^2}{N_0} \right\}. \quad (54)$$

The term C_2 in (51) does not have to be considered for the computation of $\bar{\lambda}_i$ in (54). Given $\bar{\lambda}_i$, the posterior probabilities of $p(d_i = 1|\mathbf{Y}^{(\beta)})$ and $p(d_i = 0|\mathbf{Y}^{(\beta)})$ can be computed by (43) and (44) replacing b_i and λ_i with d_i and $\bar{\lambda}_i$, respectively.

IV. DISCUSSION

A. PROPOSED APPROACH EXTENDED FOR HIGHER-ORDER MODULATION

The proposed approach can be extended for higher order modulation. Herein, we adopt 16QAM and present the LLR formulas for calculating the posterior probabilities of the index and data bits as an example of extending the proposed approach for higher-order modulation. With 16QAM, it follows that $M = 16$, $D = \log_2(16) = 4$, and $p_2 = k \times D = 12$. We define the set of 16QAM symbols as

$$\begin{aligned}\mathcal{S} = \{&s_{0,0,0,0}, s_{0,0,0,1}, s_{0,0,1,0}, s_{0,0,1,1},\\ &s_{0,1,0,0}, s_{0,1,0,1}, s_{0,1,1,0}, s_{0,1,1,1},\\ &s_{1,0,0,0}, s_{1,0,0,1}, s_{1,0,1,0}, s_{1,0,1,1},\\ &s_{1,1,0,0}, s_{1,1,0,1}, s_{1,1,1,0}, s_{1,1,1,1}\},\end{aligned} \tag{55}$$

where the values of the sixteen components in $\mathcal{S}$ are determined by Gray mapping [31]. We define $2p_2$ subsets of $\mathcal{S}$ as

$$\mathcal{S}_{i,x} = \begin{cases}\Phi_{1,x} & \text{if mod}(i, D) = 1\\ \Phi_{2,x} & \text{if mod}(i, D) = 2\\ \Phi_{3,x} & \text{if mod}(i, D) = 3\\ \Phi_{4,x} & \text{if mod}(i, D) = 0\end{cases} \tag{56}$$

for $i = 1, 2, \cdots, p_2$ and $x \in \{0, 1\}$, where

$$\begin{aligned}\Phi_{1,x} = \{&s_{x,0,0,0}, s_{x,0,0,1}, s_{x,0,1,0}, s_{x,0,1,1},\\ &s_{x,1,0,0}, s_{x,1,0,1}, s_{x,1,1,0}, s_{x,1,1,1}\},\end{aligned} \tag{57}$$

$$\begin{aligned}\Phi_{2,x} = \{&s_{0,x,0,0}, s_{0,x,0,1}, s_{0,x,1,0}, s_{0,x,1,1},\\ &s_{1,x,0,0}, s_{1,x,0,1}, s_{1,x,1,0}, s_{1,x,1,1}\},\end{aligned} \tag{58}$$

$$\begin{aligned}\Phi_{3,x} = \{&s_{0,0,x,0}, s_{0,0,x,1}, s_{0,1,x,0}, s_{0,1,x,1},\\ &s_{1,0,x,0}, s_{1,0,x,1}, s_{1,1,x,0}, s_{1,1,x,1}\},\end{aligned} \tag{59}$$

$$\begin{aligned}\Phi_{4,x} = \{&s_{0,0,0,x}, s_{0,0,1,x}, s_{0,1,0,x}, s_{0,1,1,x},\\ &s_{1,0,0,x}, s_{1,0,1,x}, s_{1,1,0,x}, s_{1,1,1,x}\}.\end{aligned} \tag{60}$$

In addition, we set the values of $Q_1, Q_2, \cdots, Q_k$ as

$$Q_{\lfloor (i+D-1)/D \rfloor} = \begin{cases}s_{d_i,d_{i+1},d_{i+2},d_{i+3}} & \text{if mod}(i, D) = 1\\ s_{d_{i-1},d_i,d_{i+1},d_{i+2}} & \text{if mod}(i, D) = 2\\ s_{d_{i-2},d_{i-1},d_i,d_{i+1}} & \text{if mod}(i, D) = 3\\ s_{d_{i-3},d_{i-2},d_{i-1},d_i} & \text{if mod}(i, D) = 0\end{cases} \tag{61}$$

for $i = 1, 2, \cdots, p_2$. Given $d_i = x$, $\mathcal{S}_{i,x}$ corresponds to the set of all symbols suitable for $Q_{\lfloor (i+D-1)/D \rfloor}$. Using the above definitions of $\mathcal{S}$ and $\mathcal{S}_{i,x}$, the LLR formula for calculating the posterior probability of an index bit is given by (42), and that for calculating the posterior probability of a data bit is given by (54).

B. COMPLEXITY ANALYSIS

The LLR formulas for calculating the posterior probabilities of the LDPC-coded index and data bits for OFDM-IM were reported in [25]. Assuming that the additive noises for the neighboring subcarriers are uncorrelated, we rewrite the LLR formula given in [25] for calculating the posterior probability of an index bit as

$$\lambda_i = \ln \frac{\sum_{\mathbf{a}_\eta \in \mathcal{A}_{b_i=1}} \sum_{\mathbf{X} \in \mathcal{X}_{\mathbf{a}_\eta}} e^{-\phi(\mathbf{a}_\eta, \mathbf{X})/N_0}}{\sum_{\mathbf{a}'_\eta \in \mathcal{A}_{b_i=0}} \sum_{\mathbf{X}' \in \mathcal{X}_{\mathbf{a}_\eta}} e^{-\phi(\mathbf{a}'_\eta, \mathbf{X}')/N_0}} \tag{62}$$

and the LLR formula given in [25] for calculating the posterior probability of a data bit as

$$\bar{\lambda}_i = \ln \frac{\sum_{\mathbf{a}_\eta \in \mathcal{A}} \sum_{\mathbf{X} \in \mathcal{X}_{\mathbf{a}_\eta, d_i=1}} e^{-\phi(\mathbf{a}_\eta, \mathbf{X})/N_0}}{\sum_{\mathbf{a}'_\eta \in \mathcal{A}} \sum_{\mathbf{X}' \in \mathcal{X}_{\mathbf{a}_\eta, d_i=0}} e^{-\phi(\mathbf{a}'_\eta, \mathbf{X}')/N_0}}, \tag{63}$$

with

$$\phi(\mathbf{a}_\eta, \mathbf{X}) = (\mathbf{Y}^\beta - \text{diag}\{\mathbf{H}^\beta\}\mathbf{X})^H (\mathbf{Y}^\beta - \text{diag}\{\mathbf{H}^\beta\}\mathbf{X}). \tag{64}$$

In the above, $\mathcal{X}_{\mathbf{a}_\eta}$ is defined as the set of all possible $\mathbf{X}$'s that contain k M-ary QAM symbols over the active subcarriers and $(n - k)$ 0's over the inactive subcarriers; $\mathcal{X}_{\mathbf{a}_\eta, b_i=x}$ is defined as the set of all possible $\mathbf{X}$'s that belong to $\mathcal{X}_{\mathbf{a}_\eta}$ and satisfy the condition of $b_i = x$. In computing $\{\lambda_i\}_{i=1}^{p_1}$ based on the LLR formula of (62) and the approximation property of (39), $3n \cdot M^k \cdot 2^{p_1} \cdot p_1$ complex multiplications (CMs), $2p_1$ real multiplications (RMs), $n \cdot M^k \cdot 2^{p_1} \cdot p_1$ complex additions (CAs), $((n-1) \cdot M^k \cdot 2^{p_1} + 2 \cdot M^k + 2^p_1 - 3) \cdot p_1$ real additions (RAs), and $2p_1$ operations of the logarithmic function are required. In computing $\{\bar{\lambda}_i\}_{i=1}^{p_2}$ based on the LLR formula of (63) and the approximation property of (39), $3n \cdot M^k \cdot 2^{p_1} \cdot p_2$ CMs, $2p_2$ RMs, $n \cdot M^k \cdot 2^{p_1} \cdot p_2$ CAs, $((n-1) \cdot M^k \cdot 2^{p_1} + M^k + 2 \cdot 2^{p_1} - 3) \cdot p_2$ RAs, and $2p_2$ operations of the logarithmic function are required. A CM is translated into 4 RMs and 2 RAs, and a CA is translated into 2 RAs [33]. Therefore, the total complexity of computing $\{\lambda_i\}_{i=1}^{p_1}$ and $\{\bar{\lambda}_i\}_{i=1}^{p_2}$ based on (62) and (63) and the approximation property of (39) amounts to $(12n \cdot M^k \cdot 2^{p_1} + 2) \cdot p$ RMs, and $((9n-1) \cdot M^k \cdot 2^{p_1} \cdot p + (p + p_1) \cdot M^k + (p + p_2) \cdot 2^{p_1} - 3p)$ RAs. In computing $\{\lambda_i\}_{i=1}^{p_1}$ based on the LLR formula of (42), $2n \cdot M \cdot 2^{p_1} \cdot p_1$ CMs, $(n \cdot M \cdot 2^{p_1} + 2) \cdot p_1$ RMs, $n \cdot M \cdot 2^{p_1} \cdot p_1$ CAs, $(2n-1) \cdot p_1$ RAs, $n \cdot M \cdot 2^{p_1} \cdot p_1$ operations of $|\cdot|^2$ are required. In computing $\{\bar{\lambda}_i\}_{i=1}^{p_2}$ based on the LLR formula of (54), $2n \cdot M \cdot 2^{p_1} \cdot p_2$ CMs, $((n-1) \cdot M \cdot 2^{p_1} + 2) \cdot p_2$ RMs, $n \cdot M \cdot 2^{p_1} \cdot p_2$ CAs, $(n \cdot 2^{p_1} + 1) \cdot p_2$ RAs, $n \cdot M \cdot 2^{p_1} \cdot p_2$ operations of $|\cdot|^2$ are required. The operation $|\cdot|^2$ is translated into 2 RMs and 1 RA [33]. Therefore, the total complexity of computing $\{\lambda_i\}_{i=1}^{p_1}$ and $\{\bar{\lambda}_i\}_{i=1}^{p_2}$ based on (42) and (54) amounts to $(11n \cdot M \cdot 2^{p_1} \cdot p - M \cdot 2^{p_1} \cdot p_2 + 2p)$ RMs and $(7n \cdot M \cdot 2^{p_1} \cdot p + (2n-1) \cdot p_1 + (n \cdot 2^{p_1} + 1) \cdot p_2)$ RAs. To illustrate the efficiency of the proposed approach compared to that of the conventional approach in [25], the decoding complexity reduction ratio (DCRR) is defined as

$$\begin{aligned}&\text{DCRR}(\%)\\ &= \left(1 - \frac{\text{Complexity of the proposed approach}}{\text{Complexity of the conventional approach}}\right) \times 100(\%),\end{aligned} \tag{65}$$

which indicates the percentage of complexity reduction obtained when replacing the conventional approach with the proposed approach. Therefore, the larger the DCRR, the

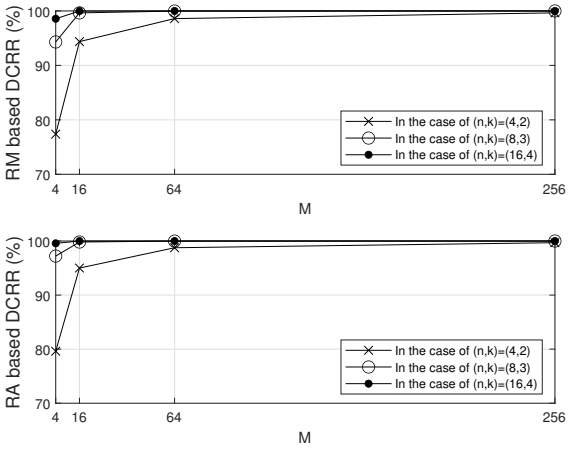

FIGURE 3. RM-based and RA-based DCRRs of the proposed approach with respect to the conventional approach in [25].

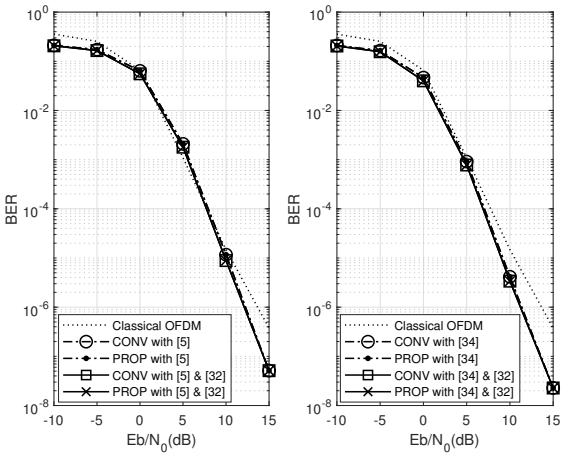

FIGURE 4. Comparison of the BER results of the proposed and conventional approaches, which were evaluated by using two index mapping methods [5] and [34] and with/without the use of the correction function [32], when $N = 128$, $L = 16$, $n = 8$, $k = 3$, $p_1 = 5$, $N_{\text{SAP}} = 56$, $N_P = 8$, and 4QAM is used.

greater the complexity reduction is obtained by the proposed approach. In Fig. 3, the RM-based and RA-based DCRRs of the proposed approach with respect to the conventional approach in [25] are plotted in three cases $(n, k) = (4, 2)$, $(n, k) = (8, 3)$, and $(n, k) = (16, 4)$. All RM-based DCRRs in the three cases are greater than 77.4% and all RA-based DCRRs in the three cases are greater than 79.6%. Both RM-based and RA-based DCRRs increase monotonously as M increases; this implies that with higher order modulation, the proposed approach can reduce the computational complexity of LDPC decoding compared to the conventional approach by a larger amount. Complexity analysis is often based on the order of the number of CMs because it is a major factor that intrinsically affects implementation complexity. Table 1 compares the number of CMs required by the proposed approach with that of CMs required by the conventional approaches in [25] and [26] when calculating the posterior probabilities of the LDPC-coded bits for a subblock. The complexity order of the proposed approach is $\mathcal{O}(M)$, whereas that of the conventional approach is $\mathcal{O}(M^k)$. Given a higher modulation order and a larger number of the active subcarriers, the proposed approach can yield a considerably lower computational complexity than that of the conventional approach.

TABLE 1. Comparison of the number of CMs required for computing the posterior probabilities of the LDPC-coded bits in a subblock.

Decoding Approach	Number of CMs	Complexity Order
Proposed	$2.5n \cdot p \cdot 2^{p_1} \cdot M$	$\mathcal{O}(M)$
Conventional ([25], [26])	$3n \cdot p \cdot 2^{p_1} \cdot M^k$	$\mathcal{O}(M^k)$

V. SIMULATION RESULTS

In Fig. 4, the BER performance of the proposed approach (PROP) and conventional approach in [25] (CONV) were evaluated for an LDPC-coded OFDM-IM system with a code rate of 0.5 when $N = 128$, $L = 16$, $n = 8$, $k = 3$, $p_1 = 5$, $N_{\text{SAP}} = 56$, $N_P = 8$, and 4QAM was used. To investigate the effect of the mapping between the ISB and SAP sequences on LDPC decoding, combinational mapping [5] and efficient index mapping [34] were applied alternately. For reference, the BER curves obtained using the correction function [32] to supplement the approximately calculated LLRs by (39) were included in the figure. While efficient index mapping improves the performance of PROP and CONV simultaneously compared to combinatorial mapping, PROP provides the same BER performance as CONV regardless of the type of mapping between the ISB and SAP sequences. Furthermore, while the correct function improves the performance of PROP and CONV simultaneously, PROP provides the same BER performance as CONV regardless of the use of the correction function. The simulation results corroborate the fact that PROP can reduce implementation complexity substantially without performance loss.

In Fig. 5, the BER performance of PROP and CONV were evaluated for an LDPC-coded OFDM-IM system with a code rate of 0.5 when the same simulation parameters as in Fig. 4 were used except that 16QAM was used in Fig. 5. To investigate the effect of the mapping between the ISB and SAP sequences on LDPC decoding, combinational mapping [5] and efficient index mapping [34] were applied alternately. For reference, the BER curves obtained using the correction function [32] were also included in the figure. Similar to Fig. 4, Fig. 5 indicates that PROP provides the same BER performance as CONV regardless of the type of mapping between the ISB and SAP sequences and the use of the correction function. The simulation results corroborate the fact that with higher-order modulation, PROP can reduce the implementation complexity by a larger amount and without performance loss.

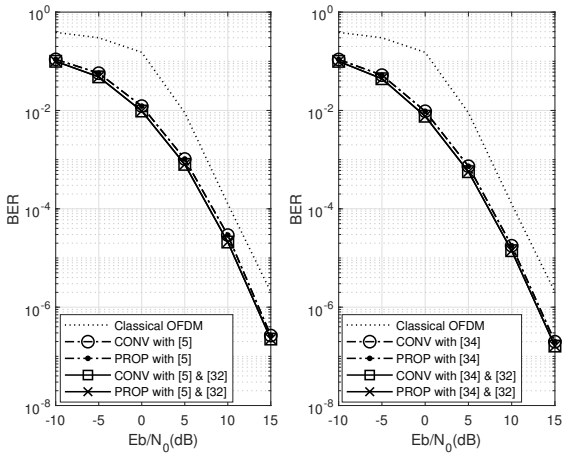

FIGURE 5. Comparison of the BER results of the proposed and conventional approaches, which were evaluated by using two index mapping methods [5] and [34] and with/without the use of the correction function [32], when $N = 128$, $L = 16$, $n = 8$, $k = 3$, $p_1 = 5$, $N_{\text{SAP}} = 56$, $N_P = 8$, and 16QAM is used.

VI. CONCLUSION

In the proposed approach, the posterior probabilities of the index and data bits were formulated as simple as possible to reduce the implementation complexity of LDPC decoding for OFDM-IM. It was demonstrated that the proposed approach can reduce the implementation complexity of LDPC decoding for OFDM-IM significantly compared to the conventional approach. The simulation results corroborated the fact that the proposed approach provides the same BER performance as the conventional approach.

REFERENCES

[1] E. Basar, M. Wen, R. Mesleh, M. D. Renzo, Y. Xiao, and H. Haas, "Index modulation techniques for next-generation wireless networks," *IEEE Access*, vol. 5, pp. 16693-16746, Sept. 2017.

[2] T. Mao, Q. Wang, Z. Wang, and S. Chen, "Novel index modulation techniques: A survey," *IEEE Commun. Surveys Tuts.*, vol. 21, no. 1, pp. 315-348, Jul. 2018.

[3] S. D. Tusha, A. Tusha, E. Basar, and H. Arslan, "Multidimensional index modulation for 5G and beyond wireless networks," *Proc. of the IEEE*, vol. 109, no. 2, pp. 170-199, Feb. 2021.

[4] P. K. Frenger and N. A. B. Svensson, "Parallel combinatory OFDM signaling," *IEEE Trans. Commun.*, vol. 47, no. 4, pp. 558-567, Apr. 1999.

[5] E. Basar, U. Aygolu, E. Panayrc, and H.V. Poor, "Orthogonal frequency division multiplexing with index modulation," *IEEE Trans. Signal Process.*, vol. 61, no. 22, pp. 5536-5549, Nov. 2013.

[6] Rui F., Ya J. Y., and Yong L. G., "Generalization of orthogonal frequency division multiplexing with index modulation," *IEEE Trans. Wireless Commun.*, vol. 14, no. 10, pp. 5350-5359, Oct. 2015.

[7] M. Wen, B. Ye, E. Basar, Q. Li, and F. Ji, "Enhanced orthogonal frequency division multiplexing with index modulation," *IEEE Trans. Wireless Commun.*, vol. 16, no. 7, pp. 4786-4801, Jul. 2017.

[8] Q. Li, M. Wen, E. Basar, H.V. Poor, B. Zheng, and F. Chen, "Diversity enhancing multiple-mode OFDM with index modulation," *IEEE Trans. Commun.*, vol. 66, no. 8, pp. 3653-3666, Aug. 2018.

[9] T. Mao, Z. Wang, Q. Wang, S. Chen, and L. Hanzo, "Dual-mode index modulation aided OFDM," *IEEE Access*, vol. 5, pp. 50-60, Feb. 2017.

[10] T. Mao, Q. Wang, and Z. Wang, "Generalized dual-mode index modulation aided OFDM," *IEEE Commun. Lett.*, vol. 21, no. 4, pp. 761-764, Apr. 2017.

[11] M. Wen, E. Basar, Q. Li, B. Zhen, and M. Zhang, "Multiple-mode orthogonal frequency division multiplexing with index modulation," *IEEE Trans. Commun.*, vol. 65, no. 9, pp. 3892-3906, Sept. 2017.

[12] Y. Xiao, S. Wang, L. Dan, X. Lei, P. Yang, and W. Xian, "OFDM with interleaved subcarrier-index modulation," *IEEE Commun. Lett.*, vol. 18, no. 8, pp. 1447-1450, Aug. 2014.

[13] E. Basar, "OFDM with index modulation using coordinate interleaving," *IEEE Wireless Commun. Lett.*, vol. 4, no. 4, pp. 381-384, Aug. 2015.

[14] Q. Li, M. Wen, B. Clerckx, S.Mumtaz, A. Al-Dulaimi, and R. Q. Hu, "Subcarrier index modulation for future wireless networks: Principles, applications, and challenges," *IEEE Wireless Commun.*, vol. 27, no. 3, pp. 1-8, Apr. 2020.

[15] Q. Ma, P. Yang, L. Dan, X. He, Y. Xiao, and S. Li, "OFDM-IM-aided cooperative relaying protocol for cognitive radio networks," in *Proc. IEEE SPAWC*, Sapporo, Japan, Jul. 3-6, 2017.

[16] Q. Li, M. Wen, S. Dang, E. Basar, H. V. Poor, and F. Chen, "Opportunistic spectrum sharing based on OFDM with index modulation," *IEEE Trans. Wireless Commun.*, vol. 19, no. 1, pp. 192-204, Jan. 2020.

[17] J. Li, Y. Peng, Y. Yan, X. Jiang, H. Hai, and M. Zukerman, "Cognitive radio network assisted by OFDM with index modulation," *IEEE Trans. Veh. Technol.*, vol. 69, no. 1, pp. 1106-1110, Jan. 2020.

[18] S. Dang, J. P. Coon, and G. Chen, "Adaptive OFDM with index modulation for two-hop relay-assisted networks," *IEEE Trans. Wireless Commun.*, vol. 17, no. 3, pp. 1923-1936, Mar. 2018.

[19] G. Sheng, S. Dang, Z. Zhang, E. Kocan, and M. Pejanovic-Djurisic, "OFDM with index modulation assisted by multiple amplify-and-forward relays," *IEEE Wireless Commun. Lett.*, vol. 8, no. 3, pp. 789-792, Jun. 2019.

[20] Z. Wang, S. Dang, and D. T. Kennedy, "Multi-hop index modulation-aided OFDM with decode-and-forward relaying," *IEEE Access*, vol. 6, pp. 26457-26468. Jun. 2018.

[21] M. Wen, X. Chen, Q. Li, E. Basar, Y. Wu, and W. Zhang, "Index modulation aided subcarrier mapping for dual-hop OFDM relaying," *IEEE Trans. Commun.*, vol. 67, no. 9, pp. 6012-6024, Sept. 2019.

[22] E. Basar, "Multiple-Input Multiple-Output OFDM with Index Modulation," *IEEE Signal Process. Lett.*, vol. 22, no. 12, pp. 2259-2263, Dec. 2015.

[23] E. Basar, "On Multiple-Input Multiple-Output OFDM with Index Modulation for Next Generation Wireless Networks," *IEEE Trans. Signal Process.*, vol. 64, no. 15, pp. 3868-3878, Aug. 2016.

[24] B. Zheng, M. Wen, E. Basar, and F. Chen, "Multiple-input multiple-output OFDM with index modulation: low-complexity detector design," *IEEE Trans. Signal Process.*, vol. 65, no. 11, pp. 2758-2772, Jun. 2017.

[25] H. Zhang, L. Yang, and L. Hanzo, "LDPC-coded index-modulation aided OFDM for in-vehicle power line communications," in *IEEE 83rd Veh. Technol. Conf. (VTC Spring)*, Nanjing, China, May 2016.

[26] X. Yu and J. Pang, "Performance evaluation of OFDM index modulation with LDPC code," in *IEEE 31st Annual Int. Symp. on Personal, Indoor and Mobile Radio Commun.*, London, UK, 31 Aug. - 3 Sept. 2020.

[27] L. Bahl, J. Cocke, F. Jelinek, and J. Raviv, "Optimal decoding of linear codes for minimizing symbol error rate," *IEEE Trans. Inf. Theory*, vol. 20, no. 2, pp. 284-287, Mar 1974.

[28] Todd K. Moon, *Error Correction Coding: Mathematical Methods and Algorithms*, Hoboken, New Jersey, USA: John Wiley & Sons, 2005.

[29] Y. Choi, P. J. Voltz, and F. A. Cassara, "On channel estimation and detection for multicarrier signals in fast and selective rayleigh fading channels," *IEEE Trans. Commun.*, vol. 49, no. 8, pp. 1375-1387, Aug. 2001.

[30] S. Song and A. C. Singer, "Pilot-aided OFDM channel estimation in the presence of the guard band," *IEEE Trans. Commun.*, vol. 55, no. 8, pp. 1459-1465, Aug. 2007.

[31] F. Gray, "Pulse code communications," U.S. Patent 2 632 058, Mar. 17, 1953.

[32] P. Robertson, E. Villebrun, and P. Hoeher, "A comparison of optimal and sub-optimal MAP decoding algorithms operating in the log domain," in *Proc. IEEE Int. Conf. on Commun. ICC '95*, Seattle, USA, 18-22 Jun. 1995.

[33] E. Hong, H. Kim, K. Yang, and D. Har, "Pilot-aided side information detection in SLM-based OFDM systems," *IEEE Trans. Wireless Commun.*, vol. 12, no. 7, pp. 3140-3147, Jul. 2013.

[34] E. Yoon, S. Kim, S. Kwon, and U. Yun, "An efficient index mapping algorithm for OFDM-index modulation," *IEEE Access*, vol. 7, pp. 184194-184206, Dec. 2019.

This article has been accepted for publication in a future issue of this journal, but has not been fully edited. Content may change prior to final publication. Citation information: DOI 10.1109/ACCESS.2021.3077256, IEEE Access

EUNCHUL YOON received the B.S. and M.S. degrees in electronics engineering from Yonsei University, Seoul, Korea, in 1993 and 1995, respectively, and the Ph.D. degrees in electronics engineering from Stanford University, CA, U.S.A in 2005. From February 1995 to July 2000, he was with the Samsung CDMA System Development team, Seoul, Korea; he was involved in the design of system software. From December 2005 to February 2008, he was with the Samsung WiMAX system development group, Suwon, Korea, where he developed the modem methods for beamforming and MIMO. He has been with the Department of Electrical and Electronics Engineering at Konkuk University, Seoul, Korea since March 2008. His research interests include wireless networks, coding and modulation, interference cancelation, and deep learning for wireless communications.

SOONBUM KWON is a graduate student at the Department of Electrical and Electronics Engineering at Konkuk University, Seoul, Korea. His research interests include wireless networks, coding and modulation, interference cancelation, and deep learning for wireless communications.

UNIL YUN received the M.S. degree in computer science and engineering from Korea University, Seoul, Korea, in 1997, and the Ph.D. degree in computer science from Texas A&M University, Texas, USA, in 2005. He worked at Multimedia Laboratory, Korea Telecom, from 1997 to 2002. After receiving Ph.D. degree, he worked as a post-doctoral associate for almost one year at the Computer Science Department of Texas A&M University. Next, he worked as a senior researcher in Electronics and Telecommunications Research Institute (ETRI). In March 2007, he joined School of Electrical & Computer Engineering of Chungbuk National University, Korea. Since August 2013, he has been with the Department of Computer Engineering at Sejong University, Seoul, Korea. His research interests include data mining, information retrieval, database systems, artificial intelligence, and digital libraries.

SUN-YONG KIM received the B.S.E. (summa cum laude), M.S.E., and Ph.D. degrees in electrical engineering from Korea Advanced Institute of Science and Technology (KAIST), Daejeon, in 1990, 1993, and 1995, respectively. From April 1995 to March 1996, he was a Visiting Researcher at the University of Tokyo, Tokyo, Japan. From March 1996 to August 2001, he was with the Department of Electronics Engineering, Hallym University. He joined the Department of Electrical and Electronics Engineering, Konkuk University in September 2001, where he is currently a Professor. He is a senior member of the Institute of Electrical and Electronics Engineers (IEEE). He won the Second-Best Paper Award from the IEEE Korea Section in 1990, a scholarship from the IEEE Communication Society in 1992-3, and a Paper Award from the LG Information and Communications in 1994. His research interests include detection and estimation theory, statistical signal processing, and analysis and design of mobile communication systems.